Shahrood University of Technology
Iranian Society of Mining Engineering (IRSME)
Journal of Mining and Environment (JME)
journal homepage: www.jme.shahroodut.ac.ir
THOMSON REUTERS
Vol. 10, No. 4, 2019, 967-978.
DOI: 10.22044/jme.2019.8501.1728

Effects of number of freeze-thaw cycles and freezing temperature on mode I and mode II fracture toughness of cement mortar

K. Abdolghanizadeh[1], M. Hosseini[1*] and M. Saghafiyazdi[2]

1. Department of Mining Engineering, College of Engineering, Imam Khomeini International University, Qazvin, Iran
2. Department of Materials Engineering, College of Engineering, Imam Khomeini International University, Qazvin, Iran

Received 29 May 2019; received in revised form 5 July 2019; accepted 15 July 2019

Keywords

Freeze-Thaw Cycle

Mode I Fracture Toughness

Mode II Fracture Toughness

Freezing Temperature

Cement Mortar

Abstract

Natural and artificial materials including rocks and cement-based materials such as concrete and cement mortar are affected both physically and chemically by various natural factors known as weathering factors. The freeze-thaw process, as a weathering factor, considerably affects the properties of rocks and concrete. Therefore, the effect of the freeze-thaw process on the physical and mechanical properties of materials should be taken into account in areas with the risk of this process. Given that few studies have been conducted on the effect of the freeze-thaw process on the fracture toughness, in this work, we aimed at investigating the effects of the freeze-thaw cycles and freezing temperature on the mode I and mode II fracture toughness of cement mortar. To this end, specimens were exposed to 0, 5, 10, 20, and 30 freeze-thaw cycles, and the mode I and mode II fracture toughness was determined in different cycles. The effect of freezing temperature in a freeze-thaw cycle on the mode I and mode II fracture toughness was also investigated. The damage factor was also defined based on the effective porosity of cement mortar, and its changes with the number of freeze-thaw cycles and mode I and mode II fracture toughness were studied. Finally, the decay function model provided by Mutluturk was investigated. According to the results obtained, the mode I and mode II fracture toughness of cement mortar decreased linearly with increase in the number of freeze-thaw cycles. The mode I and mode II fracture toughness decreased linearly with increase in the freezing temperature in a freeze-thaw cycle. The damage factor increased with increase in the number of freeze-thaw cycles, and, additionally, its relationship with mode I and mode II fracture toughness exhibited a linear behavior.

1. Introduction

The freeze–thaw process is one of the main causes of concrete deterioration in cold regions, where water periodically freezes and thaws inside the concrete during the freeze and thaw cycles, respectively. The water phase change causes a change in the internal stress of the concrete and/or the cement mortar, and eventually leads to cement fracture [1]. Freezing in porous materials such as concrete and cement mortar occurs when water molecules inside the microcracks are converted to ice, consequently increasing the volume of water molecules by 9% [2]. This, in turn, causes a tensile stress, which increases the size of cracks [3] and reduces the mechanical performance of materials. Crack propagation in rock materials is presumably the major mechanism affecting the cement-based materials during freezing [4].
Cement mortar is extensively used in bridges, water reservoirs, and silos for filling cracks in old concretes and injection in rocks [5]. Cement mortar is also used to make artificial sandstones in the study of oil wells in sandstone reservoirs [6].
Various studies have been conducted on the effect of the freeze–thaw process on concrete and

Corresponding author: ma.hosseini@eng.ikiu.ac.ir (M. Hosseini).

cement mortar-based materials. Saito *et al*. studied the effect of freeze–thaw process on chloride permeability of concrete and found that the permeability of concrete specimens was increased when exposed to the freeze–thaw process [7]. Jacobsen *et al.* examined the density and the pattern of cracks formed in the freeze–thaw process by examining thin cross-sections under a fluorescence microscope [8]. Sun *et al*. studied damage of concretes with different strengths under the simultaneous effects of the freeze–thaw process and the compressive loading and found a larger concrete degradation rate as the number of freeze–thaw cycles increased. This negative effect was more pronounced for concretes with a lower strength. They also observed a reduction in the degradation rate of specimens exposed to the freeze–thaw process by adding air and steel fibers to the concrete structure [9]. Cao *et al.* examined the concrete damage during the freeze–thaw process by measuring the electrical resistivity, and observed that the concrete damage rate was higher during the freezing cycle compared to the melting cycle. Electrical resistivity measurement allows simultaneous monitoring of temperature and damage [1]. Shang *et al.* (2006) examined the strength and deformation of concrete under triaxial stress after applying different freeze–thaw cycles. According to their results, the triaxial strength of concrete decreased with increase in the number of freeze–thaw cycles. They also provided a fracture criterion for concrete by taking into account the effect of the freeze–thaw process [10]. Siline *et al.* investigated the effect of the freeze–thaw process on cement mortar containing different amounts of pozzolan. Based on their reports, by increasing the number of freeze–thaw cycles, the uniaxial compressive strength and thermal conductivity of specimens decreased, while the porosity and water absorption increased. The presence of pozzolanic materials increases the strength of concrete against the freeze–thaw process [11]. Reis and Ferreira investigated the effect of the freeze–thaw process on the mode I fracture toughness of simple polymeric concrete and carbon and glass fiber-reinforced concretes. They found that although this toughness was not affected in simple polymeric concrete, it was decreased in carbon and fiber glass-reinforced concrete [12].

Hosseini and Khodayari investigated the effect of the freeze–thaw process on the strength and rock strength parameters on the Lushan sandstone. According to the results obtained, an increase in the number of F-T cycles and freezing temperatures reduced the uniaxial and triaxial compressive strengths, cohesion, internal friction angle, and elastic modulus due to the growth of the existing cracks and the nucleation of new cracks in the rock. Consequently, the effective porosity increased, whereas the dry specific gravity decreased with more F-T cycles and lower freezing temperatures [13].

Most studies in this area have focused on characteristics such as uniaxial and triaxial compressive strength, porosity, tensile strength, and various additives to reduce the effect of the freeze–thaw process on concrete, while few studies have investigated the effect of the freeze–thaw process on the mode I and mode II fracture toughness of concrete. This parameter is highly important in designing and analyzing the stability of concrete and cement mortar structures. Therefore, this work aimed at investigating the impact of the freeze–thaw process on the mode I and mode II fracture toughness of cement mortar using the chevron notched Brazilian disc (CCNBD) method. To this end, 0, 5, 10, 20, and 30 freeze–thaw cycles were applied to the specimens, and the mode I and mode II fracture toughness was determined in different cycles. In order to evaluate the effect of the freezing temperature on the mode I and mode II fracture toughness, the freeze–thaw experiments were carried out at -16, -20, and -24 °C on specimens that tolerated a single freeze–thaw cycle.

2. Specimens

The specimens used in the experiments were prepared from Portland cement, fine-grained sand, and water with a water-cement ratio of 0.5 and a cement-sand ratio of 1. For this purpose, the cement mortar was prepared and blended, and after pouring the mortar into the PVC pipes to create cylindrical specimens (Figure 1), the blend was mixed to let out the air bubbles of the mixture. The specimens were removed from the pipe after 24 h and stored in water. After 28 days, the physical and mechanical properties of the specimens including the effective porosity, dry weight, uniaxial compressive strength, Brazilian tensile strength, modulus of elasticity, Poisson's ratio, and adhesion were determined using the methods proposed by the International Society of Rock Mechanics (ISRM) [14]. Cores with a diameter of 59 mm and a length-diameter ratio of 2 were used for the uniaxial compressive strength test, discs with a diameter-thickness ratio of 2 for Brazilian tensile strength test, and specimens with a diameter of 54.7 mm and a length-diameter ratio of 2 for the triaxial compressive strength test. The cohesion and internal friction angles of the cement mortar specimens were determined with the help of the Rock Lab software. The saturation and immersion methods were used to measure the dry weight and effective porosity of the specimen (Table 1).

Figure 1. (a) PVC pipes for preparation of specimens; (b) specimens prepared for determination of physical and mechanical properties.

Table 1. Physical and mechanical properties of cement mortar specimen.

Dry unit weight (KN/m^3)	Effective porosity (%)	Cohesion (MPa)	Poisson's ratio	Modulus of elasticity (GPa)	Internal friction angle (°)	Brazilian tensile strength (MPa)	Uniaxial compressive strength (MPa)
18.25	12.23	2.16	0.18	20.45	36.07	4.7	29.05

3. Freeze-thaw experiment

To perform a freeze–thaw test, the specimens were first saturated in water under the ambient pressure for 48 h. The saturated specimens were exposed to a temperature of -16 °C for 18 h (freezing) and then at 20 °C for 6 h (thaw), adding up to a total of 24 h for each freeze-thaw cycle. The mode I and mode II fracture toughness of the specimens was determined prior to the freeze–thaw cycles and also after applying 5, 10, 20, and 30 freeze–thaw cycles. The freeze–thaw experiment was carried out at -16, -20, and -24 °C, and the fracture toughness was measured for a single freeze–thaw cycle to investigate the effect of the freezing temperature.

4. Fracture toughness experiment

The cracked chevron notched Brazilian disc (CCNBD) method was used to determine the mode I and mode II fracture toughness of the specimens. This method is capable of calculating the mode I and mode II fracture toughness as well as the combined fracture toughness. The geometry and loading of the Brazilian disc are depicted in Figure 2 [15].

The dimensionless parameters shown in Eq. (1) are used to describe the geometry of the chevron notch. The geometric conditions of the specimen required based on these parameters are shown in Figure 3:

$$\propto_0 = \frac{a_0}{R} \quad \propto_1 = \frac{a_1}{R} \quad \propto_B = \frac{B}{R} \quad \propto_S = \frac{D_S}{2R} \tag{1}$$

where R represents the disc radius, B is the disc thickness, and D_S ($2R_S$) is the diameter of the cutter-head.

If the notch angle (α) equals 0, the specimen is subjected to pure mode I, and the fracture toughness is calculated from Eq. (2):

$$K_{IC} = \frac{F_{Max}}{B\sqrt{D}} Y^*_{min} \tag{2}$$

where K_{IC} is the mode I fracture toughness, F_{MAX} the load at fracture, R the disc radius, B the disc thickness, and Y_{min^*} the dimensionless critical stress coefficient, which is calculated from Eq. (3):

$$Y^*_{min} = ue^{V\alpha_1} \tag{3}$$

where the constants u and v are calculated from the parameters α_0 and α_B in Table 2.
The pure mode II conditions for CCNBD are met when the angle between the notch and the loading direction is set to an appropriate size. This angle has been determined by theoretical and numerical methods. For instance, Ayatollahi and Aliha analyzed a Brazilian disc specimen by the finite element method in order to determine the angle corresponding to the pure mode II at different a/R ratios. Figure 4 shows the changes in the angle α_{II} with respect to a/R. The mode II fracture toughness is calculated from Eq. (4) [14].

$$K_{IIC} = \frac{P_{Max}}{\sqrt{\pi R}\,B} \sqrt{\frac{a}{R}} \sqrt{\frac{\alpha_1 - \alpha_0}{a - \alpha_0}} Y_{II} \tag{4}$$

where Y_{II} is the geometry factor of pure mode II (Figure 5), which depends on the crack length ratio (a/R). This geometry factor can be obtained from numerical modeling by the finite element method [16].
The geometric dimensions of CCNBD were selected considering the geometric limitations of this method (Table 3). In order to prepare the specimen, cores with a diameter of 71 mm were cut into discs of 24 mm thickness. In order to create a chevron notch, a finger milling with a special base and a cutting disc with a 40 mm diameter was used (Figure 6). To create a chevron notch on both sides of the specimen (Figure 7), two grooves with a depth of 14 mm were created at the center.

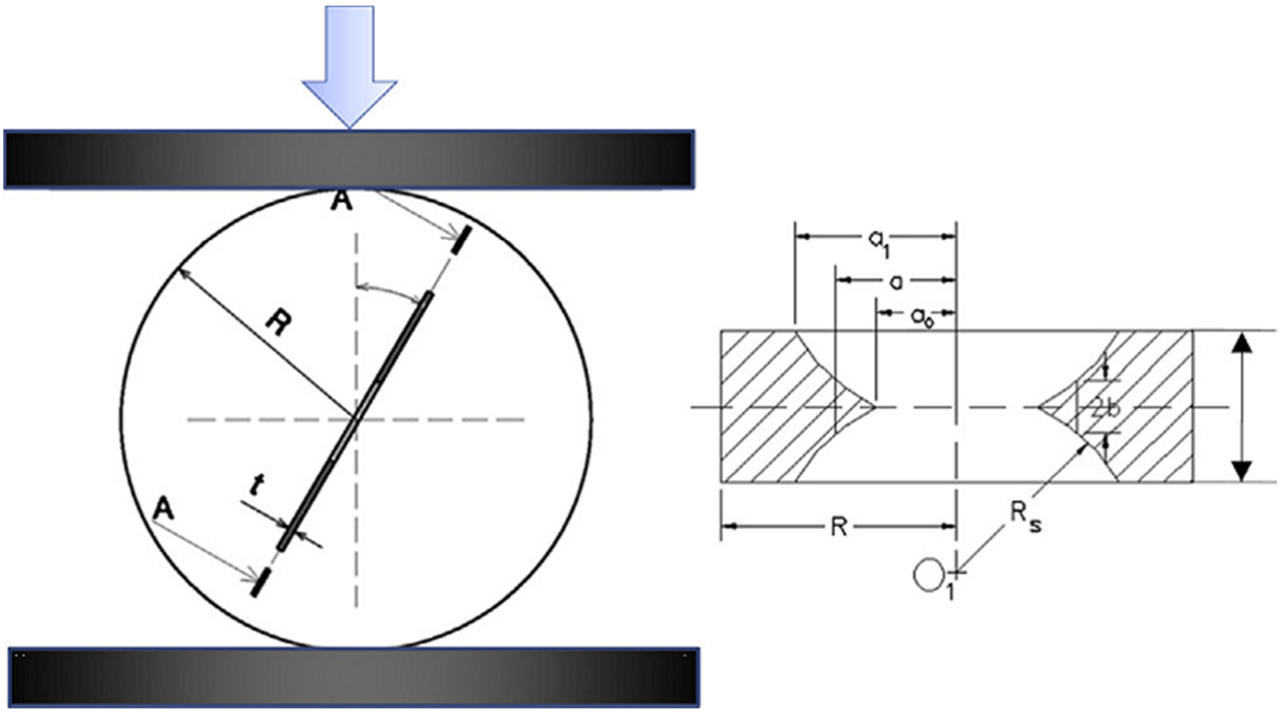

Figure 2. Geometry and loading of CCNBD [16].

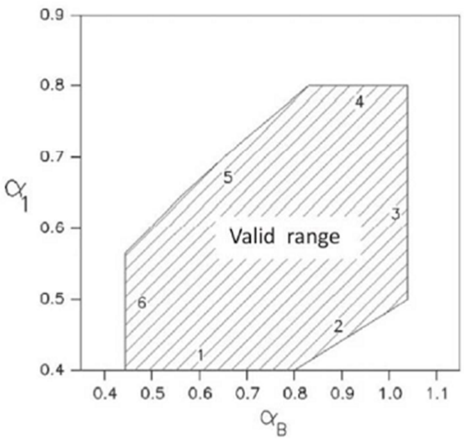

Figure 3. Geometry of CCNBD [16].

Table 2. Values of u and v for different α_0 and α_B [15].

α_0	0.200	0.250	0.275	0.300	0.325	0.350	0.375	0.400
α_B				u				
0.680	0.2667	0.2704	0.2718	0.2744	0.2774	0.2807	0.2848	0.2888
0.720	0.2650	0.2683	0.2705	0.2727	0.2763	0.2794	0.2831	0.2871
0.760	0.2637	0.2668	0.2693	0.2719	0.2744	0.2781	0.2819	0.2860
0.800	0.2625	0.2657	0.2680	0.2706	0.2736	0.2772	0.2811	0.2845
0.840	0.2612	0.2649	0.2672	0.2699	0.2727	0.2763	0.2801	0.2831
0.880	0.2602	0.2642	0.2668	0.2691	0.2723	0.2754	0.2793	0.2816
0.920	0.2598	0.2634	0.2658	0.2684	0.2716	0.2747	0.2782	0.2811
0.960	0.2593	0.2633	0.2655	0.2685	0.2710	0.2746	0.2767	0.2799
1.000	0.2591	0.2630	0.2653	0.2679	0.2709	0.2738	0.2768	0.2786
				v				
0.680	1.7676	1.7711	1.7757	1.7759	1.7754	1.7741	1.7700	1.7666
0.720	1.7647	1.7698	1.7708	1.7722	1.7693	1.7683	1.7652	1.7617
0.760	1.7600	1.7656	1.7649	1.7652	1.7662	1.7624	1.7593	1.7554
0.800	1.7557	1.7611	1.7613	1.7603	1.7596	1.7561	1.7525	1.7512
0.840	1.7522	1.7547	1.7551	1.7548	1.7535	1.7499	1.7469	1.7473
0.880	1.7487	1.7492	1.7478	1.7487	1.7463	1.7452	1.7403	1.7434
0.920	1.7423	1.7446	1.7443	1.7432	1.7411	1.7389	1.7360	1.7363
0.960	1.7370	1.7373	1.7372	1.7346	1.7344	1.7309	1.7343	1.7331
1.000	1.7308	1.7307	1.7306	1.7297	1.7273	1.7270	1.7258	1.7302

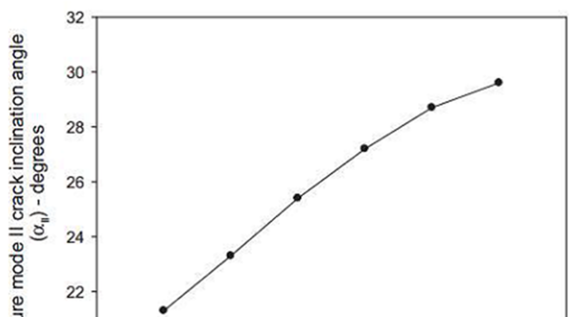

Figure 4. The angle for pure mode II corresponding to different a/R values [16].

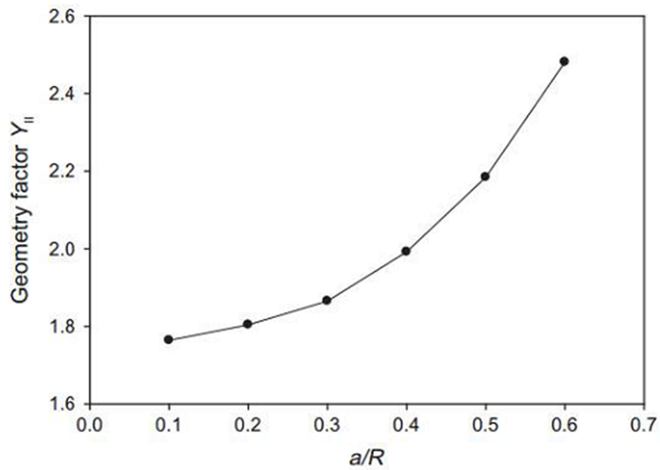

Figure 5. The geometry factor of mode II with respect to the ratio a/R for CCNBD [16].

Table 3. Geometric dimensions of the specimens prepared for determining mode I and mode II fracture toughness.

B (mm)	R_s (mm)	a (mm)	a_1 (mm)	a_0 (mm)	R (mm)	Pure mode II angle (°)
24	20	13	18.5	7.5	35.5	26.5

Figure 6. A finger milling with a special base to create a chevron notch.

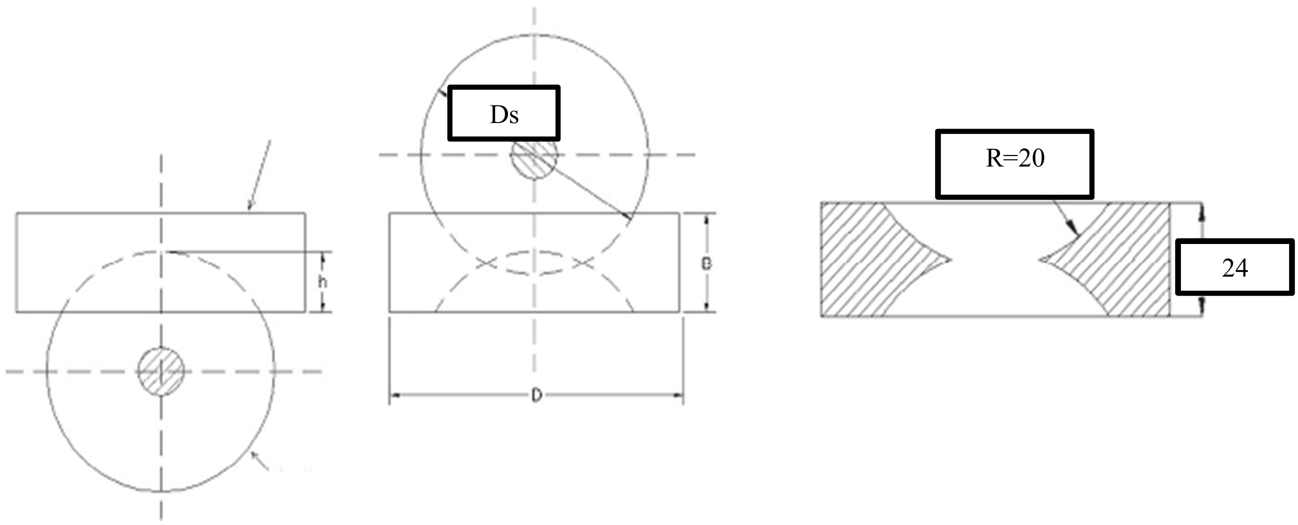

Figure 7. Steps to create a chevron notch by a 40 mm diameter disc milling [16].

5. Results and discussion

5.1. Effect of number of freeze–thaw cycles on mode I and mode II fracture toughness

The mode I and mode II fracture toughness was determined before applying the freeze–thaw cycles and after 5, 10, 20, and 30 cycles (Tables 4 and 5). Three experiments were carried out to determine the fracture toughness at each cycle. The average results are given in Tables 4 and 5.

In order to investigate the relationship between the mode I and mode II fracture toughness and the number of freeze–thaw cycles, the changes in the fracture toughness were plotted with respect to the number of cycles and the best curve fitting the points was plotted (Figures 8 and 9). As it can be clearly seen, the mode I and mode II fracture toughness decreases linearly with a coefficients of determination of 0.98 and 0.82, respectively, as the number of freeze–thaw cycles increases.

Calculated by Eq. (5), the reductions in mode I and mode II fracture toughness after the end of 30 cycles were 22.38% and 14.82%, respectively. As shown, the mode II fracture toughness shows a lower reduction than mode I fracture toughness, indicating the less impact of the freeze–thaw cycles on the mode II fracture toughness as compared to the mode I fracture toughness.

$$R = \frac{K_{I_0} or K_{II_0} - K_{I_{30}} or K_{II_{30}}}{K_{I_0} or K_{II_0}} \times 100 \tag{5}$$

where K_{I0} is the mode I fracture toughness before applying the freeze-thaw cycle, K_{I30} the mode I fracture toughness after 30 cycles, K_{II0} the mode II fracture toughness before applying the freeze-thaw cycles, K_{II30} the mode II fracture toughness after 30 cycles, and R is the percentage changes in the mode I and mode II fracture toughness after applying 30 freeze–thaw cycles.

Table 4. Mode I fracture toughness of cement mortar before applying freeze-thaw cycles and after 5, 10, 20, and 30 cycles.

Number of cycles	Mode I fracture toughness (MPa.m$^{1/2}$)
0	0.335
5	0.32
10	0.31
20	0.275
30	0.26

Table 5. Mode II fracture toughness of cement mortar before applying freeze-thaw cycles and after 5, 10, 20, and 30 cycles.

Number of cycles	Mode II fracture toughness (MPa.m$^{1/2}$)
0	0.73
5	0.72
10	0.68
20	0.69
30	0.59

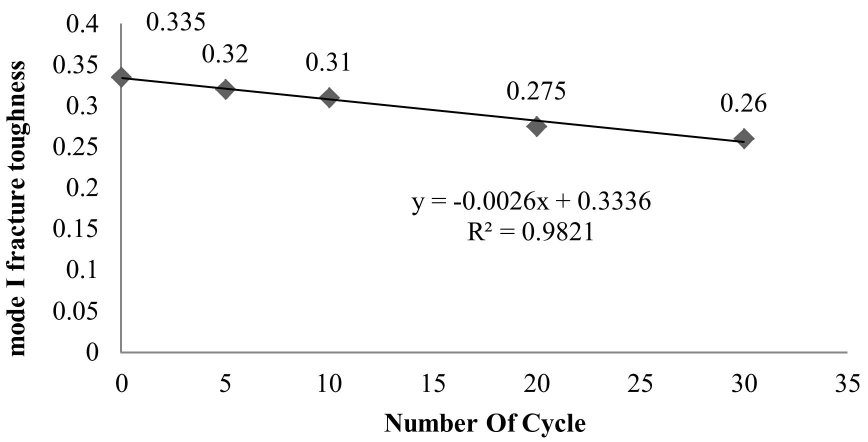

Figure 8. Mode I fracture toughness versus number of freeze–thaw cycles (the points show the mean value of the mode I fracture toughness after 0, 5, 10, 20, and 30 cycles).

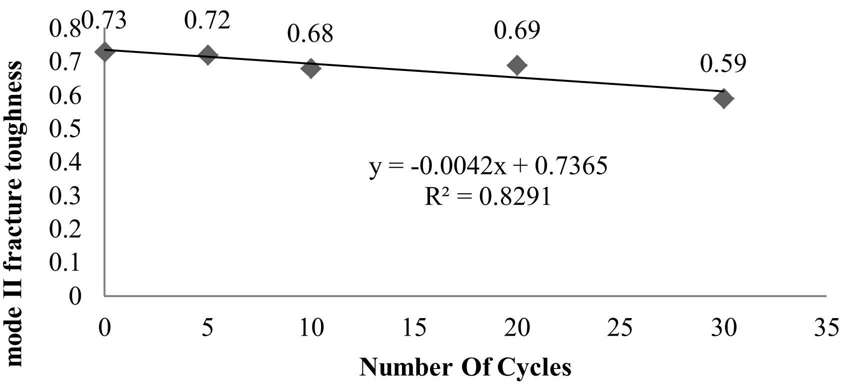

Figure 9. Mode II fracture toughness versus number of freeze–thaw cycles (the points show the mean value of the mode II fracture toughness after 0, 5, 10, 20, and 30 cycles).

5.2. Effect of freezing temperature on freeze–thaw process

As mentioned earlier, the cement mortar specimens were exposed to the different temperatures of -16, -20, and -24 °C during the freezing step of a freeze-thaw cycle to study the effect of the freezing temperature on the mode I and mode II fracture toughness. The results obtained were plotted as the fracture toughness (modes I and II) versus the freezing temperature in Figures 10 and 11 (three fracture toughness tests were carried out at each temperature and the mean values were displayed on the diagrams).

As it can be clearly seen, the mode I and mode II fracture toughness of cement mortar linearly decrease with a coefficient of determination of 0.93 and 0.90, respectively, as the freezing temperature in the freeze–thaw process increases.

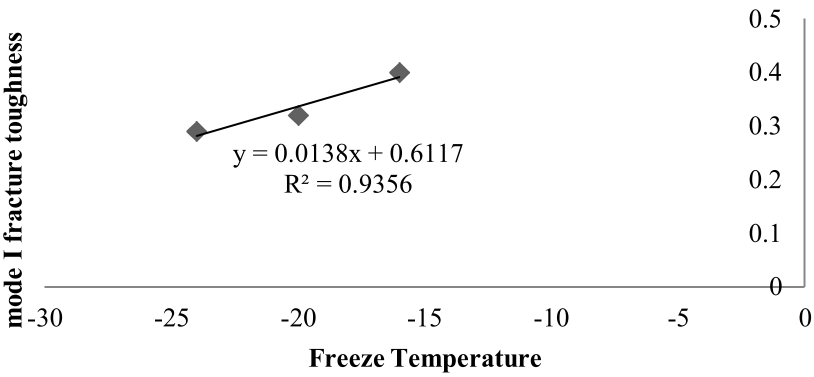

Figure 10. Mode I fracture toughness of cement mortar with respect to freezing temperature (the marked points show the mean mode I fracture toughness at -16, -20, and -24 °C).

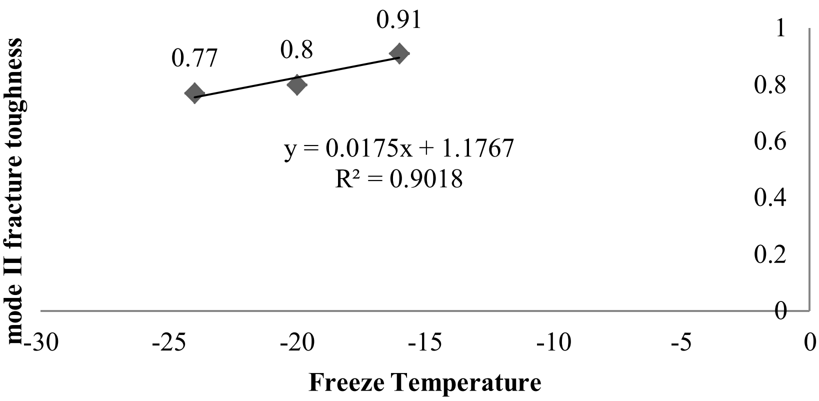

Figure 11. Mode II fracture toughness of cement mortar with respect to freezing temperature (the marked points show the mean mode II fracture toughness at -16, -20, and -24 °C).

5.3. Degradation mechanism

To investigate the degradation mechanism, the damage factor D was calculated from Eq. (6) based on the change in the effective porosity before applying the freeze–thaw cycles and after 5, 10, 20, and 30 cycles (Table 6). The damage factor is displayed in Figure 12 with respect to the number of freeze–thaw cycles [17].

$$D = \frac{n_N - n_0}{n_0} \tag{6}$$

where D represents the damage factor, n_N is the effective porosity after N cycles, and n_0 denotes the initial porosity.

As shown in Figure 12 and based on Eq. (7), with increase in the number of freeze–thaw cycles, the damage factor linearly increases with a coefficient of determination (R^2) of 0.96, which indicates the formation and development of cracks in the specimen.

The relationships between the damage factor and mode I and mode II fracture toughness of cement mortar are shown in Figures 13 and 14.

As it can be clearly seen, with increase in the damage factor, the mode I and mode II fracture toughness decrease linearly with a coefficients of determination of 0.96 and 0.75 based on Eqs. (8) and (9), respectively.

$$D = 0.018\text{N} + 0.0241 \tag{7}$$

$$K_{ICN} = \text{-}0.1398\text{D} + 0.336 \tag{8}$$

$$K_{IICN} = \text{-}0.2177\text{D} + 0.7381 \tag{9}$$

Table 6. The effective porosity percentage of cement mortar specimens before applying freeze–thaw cycles and after 5, 10, 20, and 30 cycles.

Number of cycles	Effective porosity (%)	D
0	12.23	0
5	13.25	0.08
10	15.42	0.26
20	17.35	0.41
30	18.67	0.52

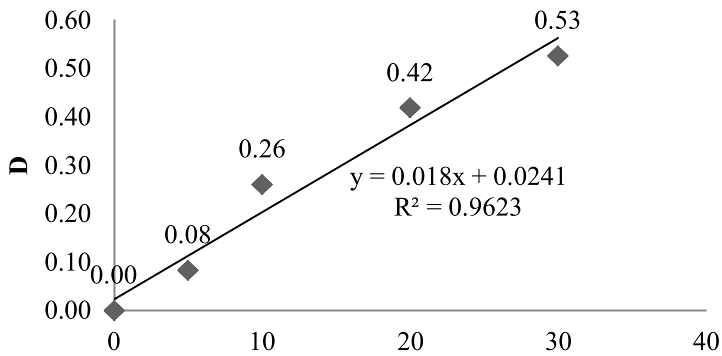

Figure 12. Damage factor as a function of the number of freeze–thaw cycles.

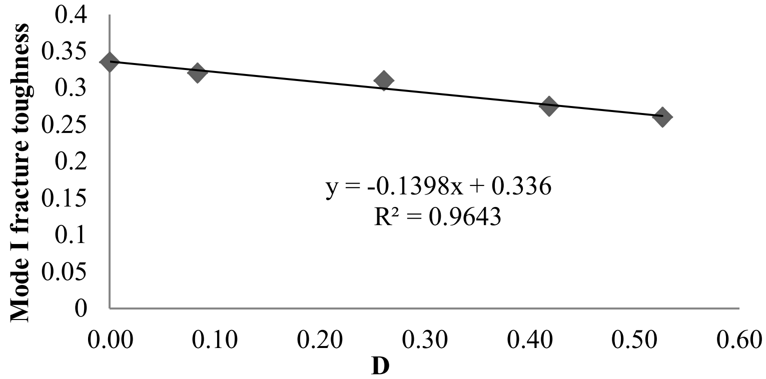

Figure 13. Mode I fracture toughness versus damage factor.

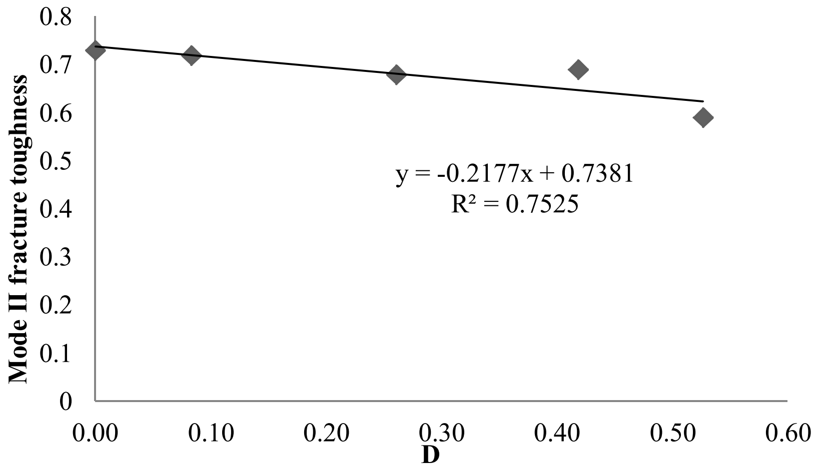

Figure 14. Mode II fracture toughness versus damage factor.

5.4. Evaluation of decay function model

The decay function model was first introduced by Mutluturk in order to predict the effect of the number of freeze–thaw and heing–cooling cycles on the rock integrity. In this model, the rock integrity reduction due to freeze–thaw and heating–cooling cycles is modeled as a first-order process and the degradation rate due to these processes is assumed proportional to the rock integrity at the beginning of each cycle, as expressed in Eq. (10) [18]:

$$-\left\{ {dI}/{dN} \right\} = \lambda I \tag{10}$$

where {dI/dN} is the degradation (decay) rate, λ the decay constant, I the rock integrity, and N the number of cycles. The exponential relation in Eq. (11) is obtained by integrating Eq. (9):

$$I_N = I_0 e^{-\lambda N} \tag{11}$$

where λ is the decay constant, N the number of cycles, I_N the rock integrity after N cycles, and I_0 the initial rock integrity before applying the cycle. In this work, another relationship known as "rock half-life" was defined as a measure of rock durability. By definition, rock half-life is the number of cycles required to reduce the rock integrity by 50% based on Eq. (12):

$$N_{1/2} = \frac{0.693}{\lambda} \tag{12}$$

where $N_{1/2}$ is the half-life of the rock and λ is the decay constant. The validity of the model is determined by examining the goodness of fit (GOF) of the experimental data. For this purpose, an exponential relationship was derived between the number of cycles and the mode I and mode II fracture toughness, as shown in Figures 15 and 16. GOF of the decay function model is determined by the coefficient of determination (R^2). As shown, the coefficients of determination for the Mutluturk decay function model for the modes I and II fracture toughness are, respectively, 0.98 and 0.81, indicating the high validity of this model for the results of this work. The decay constant and half-life of cement mortar for the mode I and mode II fracture toughness are listed in Table 7 based on the Mutluturk decay function model.

As it can be clearly seen, the half-life of the mode II fracture toughness of the cement mortar is greater than that of the mode I, indicating the lower impact of the number of freeze–thaw cycles on the mode II facture toughness of the cement mortar.

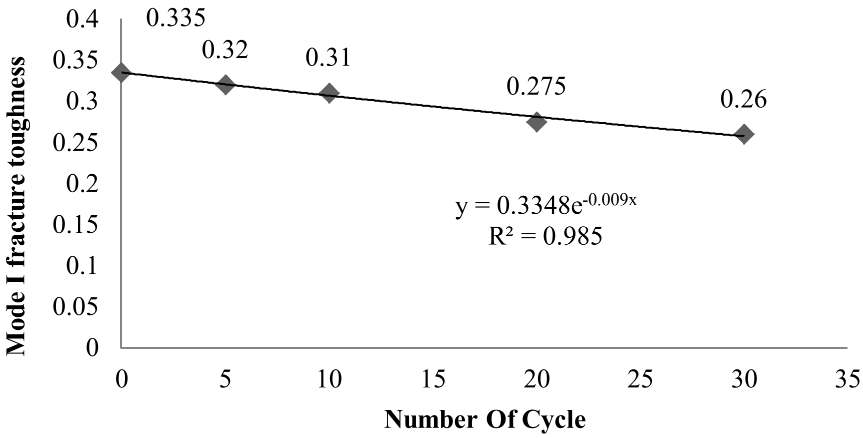

Figure 15. Mode I fracture toughness versus number of cycles in the form of Mutluturk decay function model.

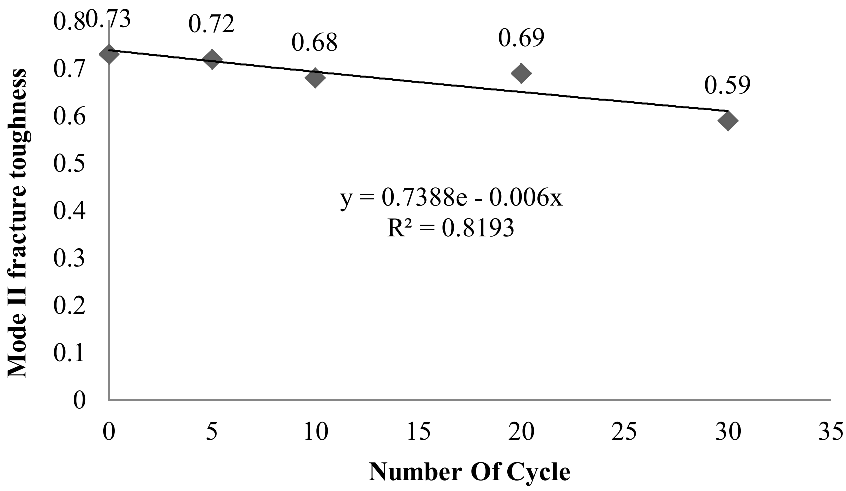

Figure 16. Mode II fracture toughness versus number of cycles in the form of Mutluturk decay function model.

Table 7. Half-life and decay constant of modes I and mode II fracture toughness of cement mortar.

Parameter	Half-life	Decay constant
Mode I fracture toughness	77	0.009
Mode II fracture toughness	116	0.006

6. Conclusions

The effects of the number of freeze–thaw cycles and freezing temperature in a freeze–thaw cycle on the mode I and mode II fracture toughness of cement mortar was investigated. To this end, 0, 5, 10, 20, and 30 freeze–thaw cycles were applied to the cracked chevron notched Brazilian disc (CCNBD) specimens, and the mode I and mode II fracture toughness was determined. The damage factor was expressed as a function of the effective porosity, and its relationship with the changes in fracture toughness was investigated. Finally, the decay function model presented by Mutluturk was evaluated. The results obtained showed that:

- The mode I fracture toughness of cement mortar decreased linearly with increase in the number of freeze–thaw cycles with a coefficient of determination of 0.98. The mode I fracture toughness decreased by 22.38% after the end of 30 cycles.
- The mode II fracture toughness of cement mortar decreased linearly with increase in the number of freeze–thaw cycles with a coefficient of determination of 0.82. The mode II fracture toughness decreased by 14.82% after the end of 30 cycles.
- The percentage reduction in the mode II fracture toughness at the end of the 30 cycles was less than that of the mode I fracture toughness, indicating the lower impact of the freeze–thaw process on the mode II fracture toughness.

- The mode I and mode II fracture toughness of cement mortar decreased linearly with coefficients of determination of 0.93 and 0.90, respectively.
- By increasing the number of cycles, the damage factor defined based on the porosity of the cement mortar increased linearly with a coefficient of determination of 0.94, indicating the formation and development of various cracks in the specimen due to the freeze–thaw process.
- A linear relationship was found between the damage factor and the mode I and mode II fracture toughness with coefficients of determination of 0.96 and 0.75, respectively. The mode I and mode II fracture toughness of the cement mortar decreased with increase in the damage factor.
- Given the high reliability and goodness of fit (GOF) using the Mutluturk decay function model, this model can be reliably used to predict the long-term effect of the number of freeze–thaw cycles on the cement mortar.

References

[1]. Cao, J. and Chung, D.D.L. (2002). Damage evolution during freeze–thaw cycling of cement mortar, studied by electrical resistivity measurement. Cement and Concrete Research. 32 (10): 1657-1661.

[2]. Valenza II, J.J. and Scherer, G.W. (2007). A review of salt scaling: II. Mechanisms. Cement and Concrete Research. 37 (7): 1022-1034.

[3]. Chung, C.W., Shon, C.S. and Kim, Y.S. (2010). Chloride ion diffusivity of fly ash and silica fume concretes exposed to freeze–thaw cycles. Construction and Building Materials. 24 (9): 1739-1745.

[4]. Vancura, M., MacDonald, K. and Khazanovich, L. (2011). Microscopic analysis of paste and aggregate distresses in pervious concrete in a wet, hard freeze climate. Cement and Concrete Composites. 33 (10): 1080-1085.

[5]. Ohama, Y. and Ramachandran, V.S. (1996). Polymer-Modified Mortars and Concretes. In Concrete Admixtures Handbook (Second Edition), William Andrew Publishing. pp. 558-656.

[6]. Massih, A. and Moomivand, H. (2018). Making artificial sandstone with a wide range of porosities. Journal of petroleum geomechanics. 2 (1): 85-99.

[7]. Saito, M., Ohta, M. and Ishimori, H. (1994). Chloride permeability of concrete subjected to freeze-thaw damage. Cement and Concrete Composites. 16 (4): 233-239.

[8]. Jacobsen, S., Gran, H.C., Sellevold, E.J. and Bakke, J.A. (1995). High strength concrete-Freeze/thaw testing and cracking. Cement and concrete research. 25 (8): 1775-1780.

[9]. Sun, W., Zhang, Y.M., Yan, H.D. and Mu, R. (1999). Damage and damage resistance of high strength concrete under the action of load and freeze-thaw cycles. Cement and Concrete Research. 29 (9): 1519-1523.

[10]. Shang, H.S. and Song, Y.P. (2006). Experimental study of strength and deformation of plain concrete under biaxial compression after freezing and thawing cycles. Cement and Concrete Research. 36 (10): 1857-1864.

[11]. Siline, M., Ghorbel, E. and Bibi, M. (2017). Effect of freeze–Thaw cycles on the physicomechanical properties of a pozzolanic mortar. Construction and Building Materials. 134: 32-38.

[12]. Reis, J.M.L. and Ferreira, A.J.M. (2006). Freeze–thaw and thermal degradation influence on the fracture properties of carbon and glass fiber reinforced polymer concrete. Construction and building materials. 20 (10): 888-892.

[13]. Hosseini, M. and Khodayari, A.R. (2019). Effect of freeze-thaw cycle on strength and rock strength parameters (A Lushan sandstone case study). Journal of Mining and Environment. 10 (1): 257-270.

[14]. Hatheway, A.W. (2009). The complete ISRM suggested methods for rock characterization, testing and monitoring. pp. 1974-2006.

[15]. Fowell, R., Hudson, J., Xu, C., Chen, J. and Zhao, X. (2007). Suggested method for determining mode I fracture toughness using cracked chevron notched Brazilian disc (CCNBD) specimens. Elsevier.

[16]. Aliha, M.R.M. and Ayatollahi, M.R. (2014). Rock fracture toughness study using cracked chevron notched Brazilian disc specimen under pure modes I and II loading–A statistical approach. Theoretical and Applied Fracture Mechanics. 69: 17-25.

[17]. Han, T., Shi, J. and Cao, X. (2016). Fracturing and Damage to Sandstone Under Coupling Effects of Chemical Corrosion and Freeze–Thaw Cycles. Rock Mechanics and Rock Engineering. 49 (11): 4245-4255.

[18]. Mutlutürk, M., Altindag, R. and Türk, G. (2004). A decay function model for the integrity loss of rock when subjected to recurrent cycles of freezing–thawing and heating–cooling. International journal of rock mechanics and mining sciences. 41 (2): 237-244.

تأثیر تعداد سیکل‌های یخبندان- ذوب و دمای یخبندان بر روی چقرمگی شکست مود I و II ملات سیمان

کوروش عبدالغنی زاده[۱]، مهدی حسینی[۱*] و مرتضی ثقفی یزدی[۲]

۱- گروه مهندسی معدن، دانشگاه بین‌المللی امام خمینی (ره)، ایران

۲- گروه مهندسی مواد، دانشگاه بین‌المللی امام خمینی (ره)، ایران

ارسال ۲۰۱۹/۵/۲۹، پذیرش ۲۰۱۹/۷/۱۵

* نویسنده مسئول مکاتبات: ma.hosseini@eng.ikiu.ac.ir

چکیده:

عوامل مختلف طبیعی تحت عنوان عوامل هوازدگی مصالح طبیعی و مصنوعی از جمله سنگ‌ها و مصالح بر پایه سیمان مانند بتن و ملات سیمانی را به صورت فیزیکی و شیمیایی تحت تأثیر قرار می‌دهند. فرایند یخبندان- ذوب از جمله این عوامل است که به صورت گسترده خواص سنگ‌ها و بتن را تحت تأثیر قرار می‌دهد؛ بنابراین در مناطقی که احتمال رخ دادن این فرایند است ضروری است تا تأثیر این فرایند بر روی ویژگی‌های فیزیکی و مکانیکی مصالح در نظر گرفته شود. با توجه به این‌که پژوهش‌های بسیار کمی بر روی تأثیر یخبندان- ذوب بر روی چقرمگی شکست انجام شده است، در این پژوهش تأثیر سیکل‌های یخبندان- ذوب و تأثیر دمای یخبندان روی چقرمگی شکست مود I و II ملات سیمان مورد بررسی قرار گرفته شده است. برای این منظور نمونه‌ها تحت تأثیر ۰، ۵، ۱۰، ۲۰ و ۳۰ سیکل یخبندان- ذوب قرارگرفته و چقرمگی شکست مود I و II در سیکل‌های مختلف مورد بررسی قرار گرفته شده است. در ضمن تأثیر دمای یخبندان در یک سیکل یخبندان- ذوب بر چقرمگی شکست مود I و II بررسی شده است. همچنین فاکتور آسیب بر اساس تخلخل مؤثر ملات سیمان تعریف و رابطه تغییرات آن نسبت به تعداد سیکل‌های یخبندان- ذوب با تغییرات چقرمگی شکست مود I و II بررسی شده است و در آخر مدل تابع تخریب ارائه شده توسط موتلتورک مورد بررسی قرار گرفته شده است. نتایج نشان داده است که با افزایش تعداد سیکل‌های یخبندان- ذوب مقادیر چقرمگی شکست مود I و II ملات سیمان به صورت خطی کاهش پیدا کرده است و در یک سیکل یخبندان- ذوب با افزایش دمای یخبندان، چقرمگی شکست مود I و II نمونه‌ها به صورت خطی کاهش پیدا کرده است. همچنین با افزایش تعداد سیکل یخبندان- ذوب فاکتور آسیب افزایش پیدا کرده و رابطه آن با چقرمگی شکست مود I و II به صورت خطی است.

کلمات کلیدی: سیکل یخبندان- ذوب، چقرمگی شکست مود اول، چقرمگی شکست مود دوم، دمای یخبندان، ملات سیمان.